Journal of Applied Mechanics and Technical Physics, Vol. 50, No. 4, pp. 661–669, 2009

MODELING OF THE DIFFERENTIAL ROTATION EFFECT IN COMPLEX LOADING OF GRANULAR MEDIA

E. I. Kraus,[1] **S. V. Lavrikov,**[2] **A. E. Medvedev,**[1]
A. F. Revuzhenko,[2] **and I. I. Shabalin**[1]

UDC 539.3

A plane problem of directed mass transfer in a granular medium, induced by complex loading with continuous rotation of the principal axes of the strain tensor, is considered. It is proposed to use a hypoplastic model of a granular medium and a model of similarity of a viscous incompressible fluid to describe this effect. A finite-element algorithm is developed for the hypoplastic model, and a numerical solution of a boundary-value problem is constructed. An approximate analytical solution of the initial problem is obtained for the model of similarity of a viscous incompressible fluid. Calculations of deformation kinetics are performed for both models, and the results obtained are compared with available experimental data. Both models are demonstrated to ensure a qualitative description of the deformation process and the effect of directed mass transfer observed in experiments.

Key words: *granular medium, complex loading, mass transfer, hypoplastic model, finite elements, boundary-value problem, viscosity, small parameter, differential rotation.*

1. EFFECT OF DIFFERENTIAL ROTATION

Special types of loading of inelastic solids can induce the effect of differential rotation. To elucidate the essence of this effect, let us consider plane deformation of an ellipse-shaped domain with a given constant velocity vector on the domain boundary; this vector is directed tangent to the boundary:

$$|\boldsymbol{v}| = \text{const}, \qquad \boldsymbol{v} \cdot \boldsymbol{n} = 0. \tag{1.1}$$

Here $\boldsymbol{n}$ is the normal vector to the ellipse boundary. Under such loading, the elliptical domain transforms to itself. Any material point on the boundary moves around the center over a closed elliptical trajectory. Internal points also move around the center over closed trajectories close to ellipses. The periods of rotation of internal points are found to depend on the distance $|\boldsymbol{r}|$ between these points and the center. Thus, the effect of differential rotation is observed. For an observer located at a material point on the boundary, this effect is manifested in directed mass transfer (Fig. 1). Clearly, this process depends on medium rheology, degree of ellipse compression, and loading conditions. A detailed study of the differential rotation effect is of interest for several reasons.

1. Because of the difference in the periods of rotation of internal material points, internal strains of the medium are accumulated in time and can reach arbitrarily large values. This circumstance can be used in material forming, in obtaining defect-free packings of granular materials, etc.

2. The effect of differential rotation can be used in experimental research of the constitutive equations of rheologically complicated media. It can be easily demonstrated that only a uniform distribution of strains can be

[1]Khristianovich Institute of Theoretical and Applied Mechanics, Siberian Division, Russian Academy of Sciences, Novosibirsk 630090; kraus@itam.nsc.ru; medvedev@itam.nsc.ru; shabalin@sbras.nsc.ru. [2]Institute of Mining, Siberian Division, Russian Academy of Sciences, Novosibirsk 630091; lvk@isuni.ru; revuzhenko@isuni.ru. Translated from Prikladnaya Mekhanika i Tekhnicheskaya Fizika, Vol. 50, No. 4, pp. 139–149, July–August, 2009. Original article submitted July 9, 2008.

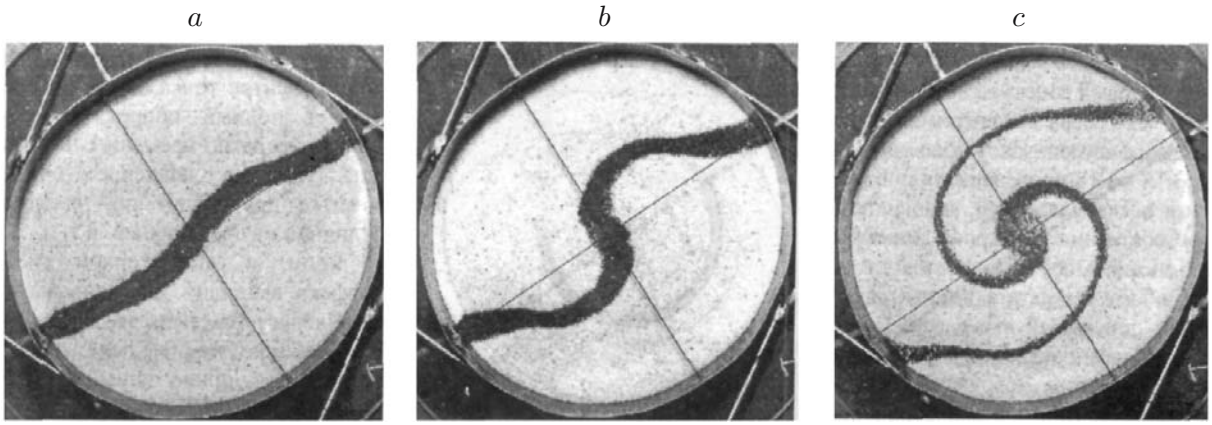

Fig. 1. Deformation pattern [1–4] obtained in experiments with dry quartz sand for an ellipse with the ratio of the major to the minor axis $\bar{a}/\bar{b} \approx 1.1$ after 3 (a), 5 (b), and 30 cycles of loading (c): the bold line is the line along the major axis of the ellipse, which was marked before deformation.

obtained if the velocity on the ellipse boundary is changed so that the sectoral velocity (rather than the absolute value of velocity $|\boldsymbol{v}|$) remains constant, i.e., the boundary conditions of the following form are imposed:

$$|\boldsymbol{v} \times \boldsymbol{r}| = \text{const}, \qquad \boldsymbol{v} \cdot \boldsymbol{n} = 0. \tag{1.2}$$

This statement is equivalent to the following. If the right end of a horizontally aligned rod is shifted to a certain distance to the right, and the left end is shifted to the same distance to the left, then the middle of the rod remains motionless (the rod material is assumed to be homogeneous and rheologically stable, and the loading process is quasi-static). The flow with a uniform distribution of strains is known to be an ideal object for geometric studies. At small coefficients of ellipse compression, the considered flows with the boundary conditions (1.1) are close to ideal flows with the boundary conditions (1.2). It is also important that the material element at the center of the elliptical domain in the steady regime experiences rigorously neutral loading: all invariants of the stress and strain-rate tensors are constant, and the loading itself is provided by rotation of the tensor axes only.

3. The above-described method of loading can be considered as kinematic modeling of the motion of tidal waves on planets. In the case considered, the observed effect implies directed transfer of the Earth's mass under the action of tidal forces.

This effect was studied in several papers [1–3, 5, 6]. In the present work, the effect of directed mass transfer is considered on the basis of two models of inelastic media.

2. PLANE BOUNDARY-VALUE PROBLEM FOR A HYPOPLASTIC MEDIUM

2.1. Hypoplastic Model. Let us consider the problem of directed mass transfer induced by complex loading within the framework of a hypoplastic model of granular media [7]. According to [4], the constitutive equations of the model relating the stress tensor T and the strain-rate tensor D have the form

$$\dot{T} = C_1 \operatorname{tr}(T+S) + C_2 \frac{\operatorname{tr}((T+S)D)}{\operatorname{tr}(T+S)}(T+S) + \Big(\frac{C_3 T^2 + C_4 T^{*^2}}{\operatorname{tr}(T)} + \frac{C_5 T^3 + C_6 T^{*^3}}{\operatorname{tr}(T^2)}\Big)\sqrt{\operatorname{tr}(D^2)}, \tag{2.1}$$

$$\dot{e} = (1+e)\operatorname{tr}(D),$$

where

$$S = sE, \qquad s = [s_0 + k(p/p_0)^\beta \ln((1+e)/(1+e_0))](p/p_0)^\alpha,$$
$$k = -s_0/[(p_r/p_0)^\beta \ln((1+e_r)/(1+e_0))], \qquad T^* = T - pE/3, \qquad p = \operatorname{tr}(T), \tag{2.2}$$

E is the unit tensor, and e is the porosity. The model constants were determined in experiments with dry quartz sand and were found to have the following values [4]:

$$C_1 = -103.01, \qquad C_2 = -197.61, \qquad C_3 = 37.24,$$

$$C_4 = 1572.92, \qquad C_5 = -394.69, \qquad C_6 = -1265.66,$$

$$p_r = -0.5 \text{ MPa}, \qquad p_0 = -0.729 \text{ MPa}, \qquad s_0 = -0.149 \text{ MPa}, \tag{2.3}$$

$$e_r = 0.73, \qquad e_0 = 0.54, \qquad \alpha = 0.6, \qquad \beta = 0.1.$$

Model (2.1)–(2.3) is an essentially nonlinear system of equations (including those for increments), which allows both the state of active loading and the state of unloading to be described within the framework of the same equations. This model was studied in numerical experiments aimed at providing a uniform stress-strain state under different types of loading. It was demonstrated that this model ensures good qualitative and quantitative descriptions of the real behavior of granular media [5].

2.2. Transition to a Two-Dimensional Problem. Equations (2.1)–(2.3) are written for a three-dimensional case. The effect of directed mass transfer, however, is observed in the plane of rotation of the principal axes of deformation. Therefore, it seems reasonable to consider a plane problem. In the case of a plane stress state, system (2.1)–(2.3) can be written in the form of a closed system of equations for the increments of the stress-tensor components $\Delta\sigma_{11}$, $\Delta\sigma_{22}$, and $\Delta\sigma_{12}$ and the field of displacements $\Delta\boldsymbol{u} = \{\Delta u_1, \Delta u_2\}$:

$$\frac{\partial\,\Delta\sigma_{11}}{\partial x_1} + \frac{\partial\,\Delta\sigma_{12}}{\partial x_2} = 0, \qquad \frac{\partial\,\Delta\sigma_{12}}{\partial x_1} + \frac{\partial\,\Delta\sigma_{22}}{\partial x_2} = 0; \tag{2.4}$$

$$\begin{aligned}
\Delta\sigma_{11} &= A_{11}\frac{\partial\,\Delta u_1}{\partial x_1} + A_{12}\Big(\frac{\partial\,\Delta u_1}{\partial x_2} + \frac{\partial \Delta u_2}{\partial x_1}\Big) + A_{13}\frac{\partial\,\Delta u_2}{\partial x_2} + A_{14}\frac{\partial\,\Delta u_3}{\partial x_3} + A_{15}\,\Delta L,\\
\Delta\sigma_{22} &= A_{21}\frac{\partial\,\Delta u_1}{\partial x_1} + A_{22}\Big(\frac{\partial\,\Delta u_1}{\partial x_2} + \frac{\partial \Delta u_2}{\partial x_1}\Big) + A_{23}\frac{\partial\,\Delta u_2}{\partial x_2} + A_{24}\frac{\partial\,\Delta u_3}{\partial x_3} + A_{25}\,\Delta L,\\
\Delta\sigma_{12} &= A_{31}\frac{\partial\,\Delta u_1}{\partial x_1} + A_{32}\Big(\frac{\partial\,\Delta u_1}{\partial x_2} + \frac{\partial \Delta u_2}{\partial x_1}\Big) + A_{33}\frac{\partial\,\Delta u_2}{\partial x_2} + A_{34}\frac{\partial\,\Delta u_3}{\partial x_3} + A_{35}\,\Delta L,\\
\Delta\sigma_{33} &= A_{41}\frac{\partial\,\Delta u_1}{\partial x_1} + A_{42}\Big(\frac{\partial\,\Delta u_1}{\partial x_2} + \frac{\partial \Delta u_2}{\partial x_1}\Big) + A_{43}\frac{\partial\,\Delta u_2}{\partial x_2} + A_{44}\frac{\partial\,\Delta u_3}{\partial x_3} + A_{45}\,\Delta L = 0,
\end{aligned} \tag{2.5}$$

$$\Delta L = \sqrt{\Big(\frac{\partial\,\Delta u_1}{\partial x_1}\Big)^2 + \frac{1}{2}\Big(\frac{\partial\,\Delta u_2}{\partial x_1} + \frac{\partial\,\Delta u_1}{\partial x_2}\Big)^2 + \Big(\frac{\partial\,\Delta u_2}{\partial x_2}\Big)^2 + \Big(\frac{\partial\,\Delta u_3}{\partial x_3}\Big)^2},$$

$$\Delta e = (1+e)\Big(\frac{\partial\,\Delta u_1}{\partial x_1} + \frac{\partial\,\Delta u_2}{\partial x_2} + \frac{\partial\,\Delta u_3}{\partial x_3}\Big).$$

Hereinafter, the quantities are normalized by the following rule: $\sigma = 10^{-1}\bar{\sigma}\rho g h$ and $s = (4/3)\bar{s}a$ (σ, s and $\bar{\sigma}$, $\bar{s}$ are the dimensional and dimensionless stress and length, respectively, ρ is the density of the medium, g is the acceleration of gravity, h is the depth of the medium layer for which the effect of differential rotation is calculated, and a is the length of the major semi-axis of the ellipse).

Equations (2.4) are the conventional equations of equilibrium for the increments of the plane stress-tensor components, and equations (2.5) are the constitutive relations of the hypoplastic model where the coefficients A_{ij} ($i = \overline{1,4}$ and $j = \overline{1,5}$) depend only on the stresses σ_{ij}, porosity e, and model constants and do not depend on the stress increments and porosity increments. In Eqs. (2.5), ΔL indicates the nonlinear part of the model equations. The equation $\Delta\sigma_{33} = 0$ serves to eliminate the quantity $\partial\,\Delta u_3/\partial x_3$, which takes into account the change in the medium volume due to deformation (dilatancy), from Eqs. (2.5).

The boundary conditions (1.1) for Eqs. (2.4) and (2.5) acquire the form

$$\Delta\boldsymbol{u}\cdot\boldsymbol{n} = 0, \qquad |\Delta\boldsymbol{u}| = d = \text{const}, \tag{2.6}$$

where d is the loading parameter.

Thus, system (2.4), (2.5) under the boundary conditions (2.6) is a closed model for calculating the increments of stresses $\Delta\sigma_{ij}$, displacements Δu_i, and porosity Δe.

To solve problem (2.4)–(2.6) numerically, we use the finite-element method (FEM). The standard FEM technique for solving boundary-value problems allows us to reduce the initial differential system of equations to a high-order algebraic system. In this case, by virtue of nonlinearity of the constitutive equations (2.5), the FEM solution is an algebraic system of nonlinear equations of the form

$$F_1(y_1, \ldots, y_m) = 0, \quad \ldots, \quad F_m(y_1, \ldots, y_m) = 0. \tag{2.7}$$

Here, the components of the vector $\boldsymbol{y} = (y_1, \ldots, y_m)$ are the increments of displacements Δu_1 and Δu_2 in nodes of a grid of finite-element splitting ($m = 2N$; N is the number of grid nodes). At each step of loading, the nonlinear system (2.7) is solved by the iterative Newton method

$$\boldsymbol{y}^{k+1} = \boldsymbol{y}^k - J^{-1}(\boldsymbol{y}^k) \cdot F(\boldsymbol{y}^k), \tag{2.8}$$

where k is the iteration number and J is the Jacobi matrix:

$$J = \begin{pmatrix} \partial F_1/\partial y_1 & \ldots & \partial F_1/\partial y_m \\ \vdots & \ddots & \vdots \\ \partial F_m/\partial y_1 & \ldots & \partial F_m/\partial y_m \end{pmatrix}.$$

The criterion of termination of the iterative process (2.8) is the condition $\max\limits_{1 \leqslant i \leqslant m} |F_i(\boldsymbol{y}^k)| < \varepsilon$ (ε is a specified small quantity). By virtue of nonlinearity of equations for increments, the global solution of the problem is constructed in the form of an iterative process as

$$\sigma_{ij}^{n+1} = \sigma_{ij}^n + \Delta\sigma_{ij}^n, \qquad u_i^{n+1} = u_i^n + \Delta u_i^n, \qquad e^{n+1} = e^n + \Delta e^n, \qquad i, j = 1, 2. \tag{2.9}$$

The increments at the nth step of loading are found by means of solving the boundary-value problem (2.4)–(2.6).

For numerical implementation of the iterative process (2.9), we have to determine the initial stress state of the medium. Experimental studies [1–3, 5, 6] showed that the deformation process reaches a steady regime, regardless of the state of the medium at the initial time. In this steady regime, all stresses do not change with time. Owing to inherent properties of granular materials, the medium become adapted to deformation conditions and "forgets" the history of its loading. In other words, the stress state in the steady regime depends only on the current loading conditions and does not depend on the stress state at the initial time. Thus, the iterative process (2.9) has to be continued until the deformation process reaches a steady regime. As a criterion of reaching this steady regime of deformation, we use a condition of the form $\max\limits_{i,j} |\Delta\bar{\sigma}_{ij}^n / \bar{d}| \ll 1$, where $\Delta\bar{\sigma}_{ij}^n$ is the increment of dimensionless stresses obtained at the nth iteration of process (2.9) and $\bar{d}$ is the dimensionless parameter of loading in the boundary condition (2.6). Thus, the criterion of reaching a steady regime of deformation implies that the calculated stress increments are close to zero, regardless of the order of smallness of the loading parameter.

A preliminary analysis of the model with uniform deformation shows that the model yields an adequate description of the process of reaching the steady regime of deformation [5]. For the case of uniform deformation [with conditions (1.2) on the external boundary], the steady state is determined rather simply, at least, there is no need to solve a boundary-value problem for that. At the same time, as was noted above, similar results are obtained for small values of ellipse eccentricity under loading conditions of the type (1.1) and (1.2). Therefore, if the state reached in the steady regime of uniform deformation with condition (1.2) on the external boundary is used as the initial stress state of the medium for problem (2.4)–(2.6), the solution obtained for the increments $\Delta\sigma_{ij}$ is expected to tend to zero, i.e., to the steady regime of deformation.

2.3. Calculation Results. Let us choose the following parameters of the computational domain and the initial stress state of the medium corresponding to the problem solution in the case of uniform deformation with conditions (1.2) on the boundary:

$$a = 130 \text{ mm}, \qquad h = 80 \text{ mm}, \qquad g = 9.81 \text{ m/sec}^2, \qquad \rho = 2.5 \text{ g/cm}^3,$$

$$\bar{a} = 0.75, \qquad \bar{b} = 0.68, \qquad e = 0.837\,11; \qquad \varepsilon = 10^{-9}, \tag{2.10}$$

$$\bar{\sigma}_{33} = -10, \qquad \bar{\sigma}_{11} = 1.25\bar{\sigma}_{33}, \qquad \bar{\sigma}_{22} = 1.19\bar{\sigma}_{33}, \qquad \bar{\sigma}_{12} = 0.7\bar{\sigma}_{33}.$$

Here $\bar{a}$ and $\bar{b}$ are the dimensionless lengths of the major and minor semi-axes of the ellipse, respectively. The stress state (2.10) is obtained as a uniform steady state of the medium by the analysis of the hypoplastic model (2.1)–(2.3).

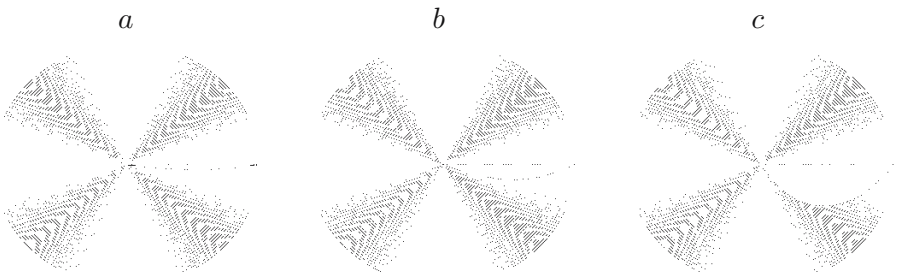

Fig. 2. Calculated pattern of deformation after 3 (a), 10 (b), and 30 (c) cycles of loading ($\bar{a}/\bar{b} \approx 1.1$).

The numerical solution of problem (2.4), (2.5) with the boundary conditions (2.6) shows that the increments of the stress-tensor components are equal to zero with a relative error of 5% already after the first iteration, i.e., $\max\limits_{i,j} |\Delta\bar{\sigma}_{ij}^n/\bar{d}| \approx 0.05$. As it could be expected, the steady state is reached after one iteration of process (2.9) with sufficient accuracy. Thus, the increment of the field of displacements $\Delta\boldsymbol{u}$ found already at the first iteration is the sought steady field of velocities formed in a granular medium under complex loading with continuous rotation of the principal axes of the strain tensor.

Based on the field found ($\Delta\boldsymbol{u}$), we construct the trajectories of motion of material points of the medium by the Euler method. The calculations show that the trajectories are closed lines whose shape is close to elliptical. The periods of rotation of different points over the trajectories constructed, however, are different. Before initiating the deformation process, we note material points lying on the major semi-axis of the ellipse. The calculations show that all internal points do not return to their initial positions after one full cycle of deformation (one complete round of the material point of the external boundary of the ellipse around the center), but they occupy some new positions. As the ellipse eccentricity is small, however, the new positions differ insignificantly from the initial ones. Nevertheless, this difference increases with increasing number of loading cycles. Figure 2 shows the initial positions, the trajectories, and the final positions of the tracked material points of the medium after the first 3, 10, and 30 cycles of loading. It is seen that the initial straight line formed by the tracked points of the major semi-axis transforms to a curve corresponding to the experimental pattern (see Fig. 1).

3. MODELING THE EFFECT OF DIFFERENTIAL ROTATION ON THE BASIS OF THE MODEL OF SIMILARITY OF A VISCOUS INCOMPRESSIBLE FLUID

The behavior of granular materials (sand) under small loading rates is known to be similar to the behavior of viscous fluids. Revuzhenko [4] described experimental results that validate the consistency in the behavior of dry quartz sand, glycerin, and honey under complex plane loading.

3.1. Equations of a Granular Medium. Under small deformations, the equations of motion of the medium (in the Cartesian coordinate system) have the form [8, 9]

$$\rho_s\tau_0\,\frac{\partial^2 u_i}{\partial t^2} = \frac{\partial\sigma_{ij}}{\partial x_j}, \qquad \sigma_{ij} = -p\delta_{ij} + 2(\mu_d + \chi_d p),$$
$$\frac{\partial u_i}{\partial x_i} = 0, \qquad \gamma_{ij} = \frac{1}{2}\Big(\frac{\partial u_i}{\partial x_j} + \frac{\partial u_j}{\partial x_i}\Big), \tag{3.1}$$

where τ_0 is the initial volume concentration of the solid phase, γ_{ij} is the strain-tensor deviator, σ_{ij} is the stress tensor, u_i are the displacements, p is the pressure in the medium, $\chi_d = \chi_d(\tau_0)$ is the dependence of the expansion coefficient on τ_0 [9], $\mu_d(\tau_0) = 2\mu_s\tau_0/(3-\tau_0)$ is the shear modulus of the porous material [10], and μ_s is the shear modulus of the solid material, $i, j = 1, 2, 3$.

The dependence of the expansion coefficient $\chi_d = \chi_d(\tau_0)$ given in [8, 9] is shown in Fig. 3. The dependence $\chi_d = \chi_d(\tau_0)$ takes into account only the re-packing of the granular medium from the minimum (cubic) packing with the concentration $\tau_0 = \pi/6 \approx 0.524$ to the maximum (tetrahedral) packing with the concentration $\tau_0 = \pi/(3\sqrt{2}\,) \approx$

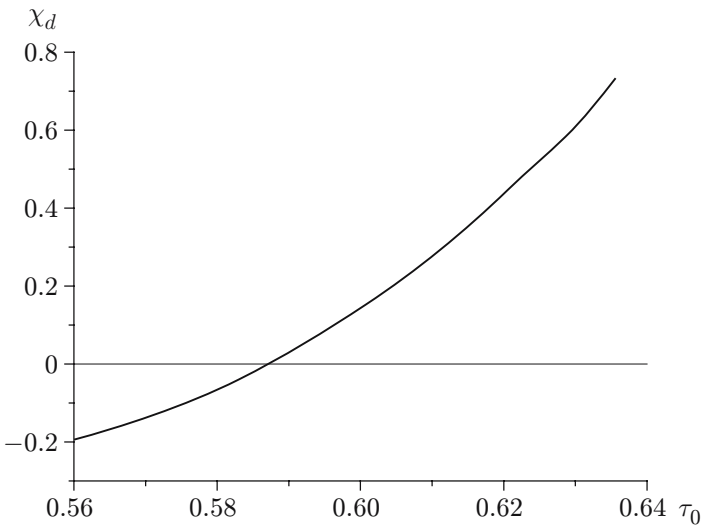

Fig. 3. Expansion coefficient χ_d versus the initial volume concentration τ_0 [9].

0.74. Deformations due to elastic compression of the particle material are added to Eqs. (3.1) (μ_d is the shear modulus of the porous material [10]). Thus, system (3.1) takes into account both the re-packing of the granular material and the elastic compression of particles.

Gol'dshtik [9] described the functional form of the dependence $\chi_d = \chi_d(\tau_0)$, but this dependence is rather complicated. Therefore, we approximate the dependence $\chi_d = \chi_d(\tau_0)$ by the quadratic formula

$$\chi_d = \chi_d(\tau_0) \approx 30.630543 - 114.207259\tau_0 + 105.654025\tau_0^2. \tag{3.2}$$

This formula yields $\chi_d = -0.1924$ for $\tau_0 = 0.56$, $\chi_d = 0$ for $\tau_0 = 0.5874$, and $\chi_d = 0.8138$ for $\tau_0 = 0.64$.

In what follows, we assume that the initial volume concentration of the solid phase is $\tau_0 = \text{const}$, i.e., the porosity $e_0 = 1 - \tau_0$ remains unchanged in the course of deformation. Granular media are known to become compacted in the course of deformation (dilatancy effect). In experiments [4, p. 59], the dilatancy effect ceases after five loading cycles: the porosity reaches a steady state with $e_0 = 0.364$ ($\tau_0 = 0.636$), while initially it was $e_0 = 0.435$ ($\tau_0 = 0.565$), and the expansion coefficient increases from $\chi_d = -0.169$ to $\chi_d = 0.731$.

3.2. Linear Approximation. In the linear approximation, system (3.1) reduced to the following system of equations [9]:

$$\nabla P = \chi_d \, \Delta \boldsymbol{u}, \qquad \operatorname{div} \boldsymbol{u} = 0. \tag{3.3}$$

Here $\boldsymbol{u}$ is the vector of displacements and $P = \ln(\chi_d p + \mu_d)$. Equations (3.3) have the form of equations of motion of a viscous incompressible fluid, written for displacements.

3.3. Equations of Motion. Let us consider complex plane deformation of the medium. In the polar coordinate system (r, φ), system (3.3) has the form

$$\frac{\partial P}{\partial r} = \chi_d\Big(\nabla^2 u - \frac{u}{r^2} - \frac{2}{r^2}\,\frac{\partial v}{\partial \varphi}\Big), \qquad \frac{1}{r}\,\frac{\partial P}{\partial \varphi} = \chi_d\Big(\nabla^2 v - \frac{v}{r^2} + \frac{2}{r^2}\,\frac{\partial u}{\partial \varphi}\Big), \qquad \frac{\partial (ur)}{\partial r} + \frac{\partial v}{\partial \varphi} = 0, \tag{3.4}$$

where $\nabla^2 = \dfrac{\partial^2}{\partial r^2} + \dfrac{1}{r}\,\dfrac{\partial}{\partial r} + \dfrac{1}{r^2}\,\dfrac{\partial^2}{\partial \varphi^2}$, u is the displacement along the normal, and v is the displacement along the tangent to the normal.

For $r = r_w$, the displacements are equal to the wall displacements along the normal and along the tangent:

$$u = \frac{\partial r_w}{\partial t}\,\Delta t, \qquad v = l\,\frac{\partial^2 r_w}{\partial t\,\partial \varphi}\,\Delta t \tag{3.5}$$

(Δt is the time step and $l = \text{const} \leqslant 1$ is the coefficient of slipping of the medium on the wall).

The following conditions should be satisfied on the cylinder axis ($r = 0$):

$$u = v = 0. \tag{3.6}$$

3.4. Cylinder Deformation. Let us consider small deformations of the wall of a cylindrical vessel (filled by a granular or viscous medium) of the form

$$r_w(t,\varphi) = r_0[1 + 0.5m\cos 2\alpha(t,\varphi)], \tag{3.7}$$

where the ellipse eccentricity m is a small parameter whose square can be neglected and $\alpha(t,\varphi) = \varphi + \pi(1-4t/t_e)/2$ [t_e is the time of the complete round of the ellipse (3.7) or the time of one loading cycle].

3.5. Introduction of Small Parameters. We apply the following transformation of variables to Eqs. (3.4):

$$t = t_e\tilde{t}, \quad r = r_0\tilde{r}, \quad u = r_0\tilde{u}, \quad v = (r_0/m)\tilde{v}, \quad P = (\chi_d/m^2)\tilde{P}. \tag{3.8}$$

In the dimensionless variables (3.8), system (3.4) acquires the form

$$\begin{gathered}
\frac{\partial\tilde{P}}{\partial\tilde{r}} = m^2\Big(\frac{\partial^2\tilde{u}}{\partial\tilde{r}^2} + \frac{1}{\tilde{r}}\,\frac{\partial\tilde{u}}{\partial\tilde{r}} + \frac{1}{\tilde{r}^2}\,\frac{\partial^2\tilde{u}}{\partial\varphi^2} - \frac{\tilde{u}}{\tilde{r}^2}\Big) - m\,\frac{2}{\tilde{r}^2}\,\frac{\partial\tilde{v}}{\partial\varphi},\\
\frac{1}{\tilde{r}}\,\frac{\partial\tilde{P}}{\partial\varphi} = m\Big(\frac{\partial^2\tilde{v}}{\partial\tilde{r}^2} + \frac{1}{\tilde{r}}\,\frac{\partial\tilde{v}}{\partial\tilde{r}} + \frac{1}{\tilde{r}^2}\,\frac{\partial^2\tilde{v}}{\partial\varphi^2} - \frac{\tilde{v}}{\tilde{r}^2}\Big) + m^2\,\frac{2}{\tilde{r}^2}\,\frac{\partial\tilde{u}}{\partial\varphi},\\
m\,\frac{\partial\tilde{u}}{\partial\tilde{r}} + \frac{1}{\tilde{r}}\,\frac{\partial\tilde{v}}{\partial\varphi} + m\,\frac{\tilde{u}}{\tilde{r}} = 0.
\end{gathered} \tag{3.9}$$

Let m be small; therefore, terms of the order of m^2 are rejected in further considerations. As a result, system (3.9) is written in the following form:

$$\begin{gathered}
\frac{\partial\tilde{P}}{\partial\tilde{r}} = -m\,\frac{2}{\tilde{r}^2}\,\frac{\partial\tilde{v}}{\partial\varphi}, \qquad \frac{1}{\tilde{r}}\,\frac{\partial\tilde{P}}{\partial\varphi} = m\Big(\frac{\partial^2\tilde{v}}{\partial\tilde{r}^2} + \frac{1}{\tilde{r}}\,\frac{\partial\tilde{v}}{\partial\tilde{r}} + \frac{1}{\tilde{r}^2}\,\frac{\partial^2\tilde{v}}{\partial\varphi^2} - \frac{\tilde{v}}{\tilde{r}^2}\Big),\\
m\,\frac{\partial\tilde{u}}{\partial\tilde{r}} + \frac{1}{\tilde{r}}\,\frac{\partial\tilde{v}}{\partial\varphi} + m\,\frac{\tilde{u}}{\tilde{r}} = 0.
\end{gathered} \tag{3.10}$$

Let $\partial\tilde{P}/\partial\tilde{r} = 0$ with accuracy to terms of the order of m^2. Then, system (3.10) in the dimensional variables (3.8) acquires the form

$$\begin{gathered}
\frac{\partial P}{\partial r} = 0, \qquad \frac{1}{r}\,\frac{1}{\chi_d}\,\frac{\partial P}{\partial\varphi} = \frac{\partial^2 v}{\partial r^2} + \frac{1}{r}\,\frac{\partial v}{\partial r} - \frac{v}{r^2},\\
\frac{\partial u}{\partial r} + \frac{1}{r}\,\frac{\partial v}{\partial\varphi} + \frac{u}{r} = 0.
\end{gathered} \tag{3.11}$$

System (3.11) has a general solution in the form

$$\begin{gathered}
u(r,\varphi) = -\frac{r}{4\chi_d}\Big[\ln\Big(\frac{r}{r_0}\Big) - 1\Big]\frac{d^2P}{d\varphi^2} - \frac{r}{2}\,\frac{dC(\varphi)}{d\varphi},\\
v(r,\varphi) = \frac{r}{4\chi_d}\Big[2\ln\Big(\frac{r}{r_0}\Big) - 1\Big]\,\frac{dP}{d\varphi} + rC(\varphi),
\end{gathered} \tag{3.12}$$

where the pressure $P(\varphi)$ and the function $C(\varphi)$ are found from the boundary conditions (3.5).

The boundary conditions (3.5) can be written as

$$u = -2\pi\,\frac{\Delta t}{t_e}\,\frac{\partial r_w}{\partial\varphi}, \qquad v = 8l\pi\,\frac{\Delta t}{t_e}\,(r_w - r_0). \tag{3.13}$$

Substituting solution (3.12) into the boundary conditions (3.13), we obtain a system of equations for the functions $P(\varphi)$ and $C(\varphi)$:

$$\begin{gathered}
\frac{\ln r_w - 1}{2\chi_d}\,\frac{d^2P}{d\varphi^2} + \frac{dC(\varphi)}{d\varphi} - 4\pi\,\frac{\Delta t}{t_e}\,\frac{\partial\ln r_w}{\partial\varphi} = 0,\\
C(\varphi) = 8l\pi\,\frac{\Delta t}{t_e}\Big(1 - \frac{1}{r_w}\Big) - \frac{2\ln r_w - 1}{4\chi_d}\,\frac{dP}{d\varphi}.
\end{gathered}$$

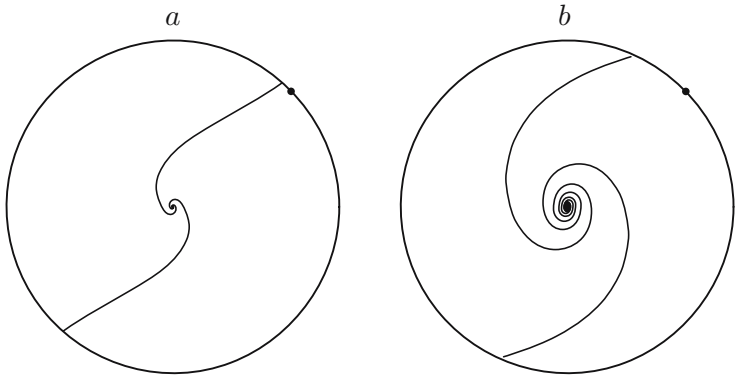

Fig. 4. Theoretical pattern of deformation after 5 (a) and 25 (b) cycles of loading: the curve shows the theoretical positions of material points that formed the major axis of the ellipse before its deformation; the point indicates the initial position of the end of the selected line on the major axis of the ellipse.

The solution of system (3.12) with the boundary conditions (3.5) and (3.6) has the following form (with accuracy to the square of the small parameter m):

$$u(t,r,\varphi) = 2\pi r(\Delta t/t_e)m[2(2l-1)\ln(r/r_0)+1]\sin 2\alpha(t,\varphi),$$

$$v(t,r,\varphi) = 4\pi r(\Delta t/t_e)m[2(2l-1)\ln(r/r_0)+l]\cos 2\alpha(t,\varphi), \tag{3.14}$$

$$P(t,\varphi) = 4\pi r(\Delta t/t_e)m(2l-1)\sin 2\alpha(t,\varphi) + P_0$$

($P_0 = \text{const}$ is the initial pressure in the medium). Solution (3.14) satisfies the boundary conditions (3.5) and (3.6).

The point with the coordinates (r_*, φ_*) moves during the time Δt to the point (r,φ) whose coordinates are determined by the formulas [11, p. 56–63]

$$r = r_* + u(t,r_*,\varphi_*), \qquad \varphi = \varphi_* + v(t,r_*,\varphi_*)/r_*.$$

3.6. Calculation Results. Solution (3.14) allows us to calculate the positions of material points of the medium in the course of its deformation. Figure 4 shows the deformation patterns calculated by Eq. (3.7) after 5 and 25 cycles of loading, which correspond to the experimental curves in Figs. 1b and 1c. The calculations were performed with the following values of parameters: radius of the non-deformed cylinder $r_0 = 20.03$ mm, ellipse eccentricity $m = \sqrt{1-(\bar{b}/\bar{a})^2} = 0.094385$ (ratio of the major to the minor semi-axis of the ellipse $\bar{a}/\bar{b} \approx 1.0045$), volume concentration of sand $\tau_0 = 0.63$ [according to Eq. (3.2), expansion coefficient $\chi_d = 0.61$], velocity of ellipse rotation $1/t_e = 3.78$ sec^{-1}, and slipping parameter $l = 0.35$. The choice of the slipping parameter $l = 0.35$ is justified by the qualitative agreement between the experimental and theoretical deformation patterns (see Figs. 1 and 4). The deformation pattern for $l = 1$ is shown in Fig. 5. It is seen that the flow pattern does not coincide with that obtained in the experiment (see Fig. 1). The effect of slipping can be attributed to flow three-dimensionality (the upper surface of the medium is the free surface), which can be taken into account by reducing the slipping parameter.

4. ANALYSIS AND COMPARISON OF RESULTS OBTAINED

Results of laboratory experiments on complex loading with continuous rotation of the principal axes of deformation for granular media, viscous fluids, and some mixtures of granular and viscous media are be found in [1–4]. If the ellipse-axes-fitted coordinate system is fixed in the course of loading, the results obtained can be interpreted as follows: all material points move over closed trajectories with different periods of rotation around the ellipse center. During the period needed for some point of the external boundary to make a complete round with respect to the center (one cycle of loading), all internal points do not complete their rotation around the center

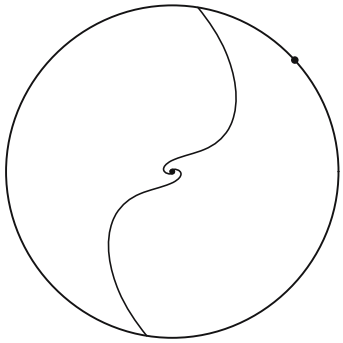

Fig. 5. Theoretical pattern of deformation after five cycles of loading with $l = 1$: the point indicates the initial position of the end of the selected line on the major axis of the ellipse.

(i.e., their motion is retarded). Thus, the effect of differential rotation, i.e., directed mass transfer is manifested. By virtue of the delay of internal points, this effect is similar to the "west drift" effect.

An analysis of results of numerical experiments on the basis of the hypoplastic model allows us to conclude that the model predicts the effect of directed mass transfer by the "west drift" type.

It follows from the present study that the model of similarity of a viscous incompressible fluid also predicts the qualitative behavior of real media. Taking into account that the degree of manifestation of the differential rotation effect in experiments strongly depends on the ellipse compression coefficient (the higher the degree of compression, the stronger the effect), we can conclude that the model of similarity of a viscous incompressible fluid predicts a more pronounced effect of differential rotation of the medium under complex loading than the hypoplastic model.

This work was supported by the Interdisciplinary Project No. 69 of the Siberian Division of the Russian Academy of Sciences.

REFERENCES

1. A. P. Bobryakov, A. F. Revuzhenko, and E. I. Shemyakin, "Possible mechanism of transfer of the Earth's mass," *Dokl. Akad. Nauk SSSR*, **272**, No. 5, 1097–1099 (1983).
2. A. F. Revuzhenko, "A class of composite loads for an inelastic material," *J. Appl. Mech. Tech. Phys.*, **27**, No. 5, 772–778 (1986).
3. A. F. Revuzhenko, "Tidal mechanism of mass transfer," *Izv. Akad. Nauk SSSR, Fizika Zemli*, No. 6, 13–20 (1991).
4. A. F. Revuzhenko, *Mechanics of Elastoplastic Media and Non-Standard Analysis* [in Russian], Izd. Novosib. Gos. Univ., Novosibirsk (2000).
5. S. V. Lavrikov and A. Ph. Revuzhenko, "Complex loading of heterogeneous materials with redistribution of internal mass," *Theor. Appl. Fracture Mech.*, **29**, 85–91 (1998).
6. D. Kolymbas, S. V. Lavrikov and A. F. Revuzhenko, "Method of analysis of mathematical models of media under complex loading," *J. Appl. Mech. Tech. Phys.*, **40**, No. 5, 895–902 (1999).
7. D. Kolymbas, I. Herle, and P.-A. von Wolffersdorff, "Hypoplastic constitutive equation with internal variables," *Int. J. Numer. Anal. Methods Geomech.*, **19**, 415–436 (1995).
8. A. M. Vaisman and M. A. Gol'dshtik, "Deformation of a granular medium," *Dokl Akad. Nauk SSSR*, **252**, No. 1, 61–64 (1980).
9. M. A. Gol'dshtik, *Transport Processes in a Granular Layer* [in Russian], Inst. of Thermophysics, Sib. Div., Acad. of Sci. of the USSR, Novosibirsk (1984).
10. S. P. Kiselev, G. A. Ruev, A. P. Trunev, et al., *Shock-Wave Processes in Two-Component and Two-Phase Media* [in Russian], Nauka, Novosibirsk (1992).
11. E. Treffz, *Mathematical Theory of Elasticity* [in Russian], ONTI, Moscow–Leningrad (1934).